frontiers | Frontiers in Marine Science

TYPE Original Research
PUBLISHED 08 May 2024
DOI 10.3389/fmars.2024.1380530

OPEN ACCESS

EDITED BY
Elva G. Escobar-Briones,
National Autonomous University of Mexico, Mexico

REVIEWED BY
Bryan O'Malley,
Eckerd College, United States
Ashley Alun Rowden,
National Institute of Water and Atmospheric Research (NIWA), New Zealand

*CORRESPONDENCE
Nene Lefaible
Nene.Lefaible@Ugent.be

RECEIVED 01 February 2024
ACCEPTED 16 April 2024
PUBLISHED 08 May 2024

CITATION
Lefaible N, Macheriotou L, Pape E, Molari M, Haeckel M, Zeppilli D and Vanreusel A (2024) Industrial mining trial for polymetallic nodules in the Clarion-Clipperton Zone indicates complex and variable disturbances of meiofaunal communities.
Front. Mar. Sci. 11:1380530.
doi: 10.3389/fmars.2024.1380530

Industrial mining trial for polymetallic nodules in the Clarion-Clipperton Zone indicates complex and variable disturbances of meiofaunal communities

Nene Lefaible[1]*, Lara Macheriotou[1], Ellen Pape[1], Massimiliano Molari[2], Matthias Haeckel[3], Daniela Zeppilli[4] and Ann Vanreusel[1]

[1]Marine Biology Research Group, Ghent University, Ghent, Belgium, [2]HGF MPG Joint Research Group for Deep Sea Ecology and Technology, Max Planck Institute for Marine Microbiology, Bremen, Germany, [3]GEOMAR Helmholtz Center for Ocean Research Kiel, Kiel, Germany, [4]UMR6197 Biologie et Écologie des Ecosystèmes Marins Profonds, University Brest, Ifremer, Plouzané, France

Following several small-scale benthic disturbance experiments, an industrial polymetallic nodule collector trial was conducted by the company Global Sea mineral Resources (GSR) in their exploration contract area in the Clarion-Clipperton Zone using the pre-prototype vehicle Patania II (PATII). In this study, meiofaunal (i.e., nematode abundance, ASV diversity and genus composition) and environmental (i.e., grain size, total organic carbon/total nitrogen and pigment) properties are compared between disturbance categories (i.e., Pre-impact, Collector Impact and Plume Impact). One week after the trial, proxies for food availability within the Collector Impact sediments were altered with lower total organic carbon (TOC) and pigment (i.e., CPE: sum of Chlorophyll *a* and phaeopigments) values. Albeit not significant, the observed decrease of nematode abundance and ASV diversity, further indicate the consequences of the removal of the ecologically important surface sediment layer within the PATII tracks. Next to sediment removal, exposed sediments were modified in different ways (e.g., central strips, parallel caterpillar imprints with alternating bands of depressions/ripples and interface patches) and were also subject to heavy collector-induced sediment blanketing. We propose that these cumulative impacts have led to intricate seabed modifications with various levels of disturbance intensity which resulted in the high meiofaunal variability observed. Adjacent nodule-rich areas (i.e., Plume Impact) received considerable levels of sediment deposition (2-3 cm) and were defined by significantly lower food sources (CPE, TOC, carbon to nitrogen ratio) and an observation of meiofaunal enrichment (i.e., higher average nematode abundance and ASV diversity; although statistically non-significant), but mechanisms behind these ecological changes (e.g., suspended material-surface fluxes, passive dispersal

of fauna in the plume vs. active upward migration and "viability" of redeposited fauna) remain unresolved. We conclude that complex benthic pressure-response relationships associated with the PATII trial, combined with the high degree of natural spatial and temporal variability in abyssal meiofaunal communities and sedimentary parameters, complicates the quantitative assessment of deep-sea mining associated disturbances.

KEYWORDS

deep-sea mining, polymetallic nodules, environmental impacts, benthic ecosystem, nematoda, metabarcoding

1 Introduction

Industrial extraction of deep-sea minerals is often put forward as a solution to provide the raw materials needed to fuel the projected future demand for metals needed for the global "green energy" transition, digitalization and future mobility (Hallgren and Hansson, 2021; Miller et al., 2021). Consequently, several countries and entrepreneurs have shown increased interests to explore certain marine areas such as the Clarion-Clipperton Zone (CCZ, eastern equatorial Pacific Ocean), where vast quantities of polymetallic nodules have been found on the abyssal seabed, rich in manganese, iron and economically important metal constituents (e.g., nickel, copper, cobalt and rare earth elements) (Broadus, 1987; Hein et al., 2013; Petersen et al., 2016). So far, a total of 17 contractors have signed exploration contracts for polymetallic nodules with the International Seabed Authority (ISA) in the CCZ (https://www.isa.org.jm/consulted on 15/09/2023) and great efforts are being made to develop the technology needed to extract these minerals in water depths exceeding 4000 m (Hein et al., 2013; Petersen et al., 2016; Sparenberg, 2019).

Because polymetallic nodules are located at the sediment-water interface, deep-sea mining (DSM) will inevitably affect overall seafloor integrity (i.e., physical, biogeochemical and biological properties) with potential long-term impacts on benthic structure and functioning (Thiel, 2001; Miljutin et al., 2011; Vanreusel et al., 2016; Jones et al., 2017; Mevenkamp et al., 2017, 2019; Volz et al., 2020; Vonnahme et al., 2020). Besides the nodule-associated fauna (e.g., sessile and mobile mega- and macrofauna but also nodule crevice meiofauna), surrounding soft-sediment habitats are also directly impacted as DSM will disturb the ecologically important surficial sediment layers by the removal of nodules and sediment combined with sediment reworking/redistribution (König et al., 2001; Stratmann et al., 2018; Haffert et al., 2020; Volz et al., 2020; Vonnahme et al., 2020). An additional stressor is the deposition of material from the suspended sediment plumes that will be created during nodule mining through the release of removed surface sediments and nodule debris behind the collector vehicle and the chain-drive of the vehicle on the seabed (Oebius et al., 2001; Muñoz-Royo et al., 2022; Gazis et al., submitted)[1]. Considering the low natural background sedimentation levels in the CCZ of less than 0.5 cm/ka (e.g., Volz et al., 2020), substantial negative effects on benthic ecosystems are expected such as altered environmental conditions (Haeckel et al., 2001; König et al., 2001; Volz et al., 2020) and (sub)lethal animal responses (e.g., behavioral changes, impaired respiration/feeding, increased mortality and toxicity) (Wilber and Clarke, 2001; Mevenkamp et al., 2017, 2019).

A full understanding of these effects is hampered by incomplete scientific baseline knowledge (Amon et al., 2022) and the fact that available data mainly come from small-scale and short-term disturbance experiments (Jones et al., 2017; Volz et al., 2018). While significant progress has been made to survey plume dispersal patterns (e.g., Gillard et al., 2019; Purkiani et al., 2021; Muñoz-Royo et al., 2022), investigating faunal responses to enhanced sediment exposure remains challenging within these areas. However, science-industry collaboration enables to investigate the nature, extent and mechanisms of DSM stressors at a representative scale (MI2, 2018; Clark et al., 2020; Amon et al., 2022). During Spring 2021, the pre-prototype nodule collector vehicle, Patania II (PATII), was successfully deployed in the Belgian (GSR) exploration contract area. PATII was able to traverse along the seabed and collect approximately 6.6 x 10^5 kg of polymetallic nodules (Gazis et al., submitted)[1].

In this study, impacts under an industry-style DSM scenario were investigated within the GSR exploration contract area with a focus on soft-sediment infauna. Sediment samples were collected within non-impacted and impacted (Collector and Plume Impact) sites. The Collector Impact site refers to the area where the PATII nodule collector removed the nodules and surface sediment, whereas the Plume Impact site refers to the area adjacent to the collector test area where the nodule habitat was blanketed by a sediment cover of 2-3 cm (Vink et al., 2022). The main objective was to assess immediate (i.e., one week after the trial) effects of nodule collection on the

1 Gazis, I. Z., de Stigter, H., Mohrmann, J., Heger, K., Diaz, M., Gillard, B., et al. (2024). Monitoring deep-sea mining benthic plumes, sediment redeposition and nodule collector imprints, [Manuscript submitted for publication].

sediment properties (i.e., grain size, total organic carbon, total nitrogen and pigments) and metazoan meiofaunal communities. Nematoda represent the dominant phylum in terms of abundance within abyssal soft sediments, typically comprising > 90% of all metazoan meiofauna, and have valuable bio-indicator properties (Rex et al., 2006; Pape et al., 2017; Hauquier et al., 2019; Hasemann et al., 2020; Danovaro and Gambi, 2022). As such, nematode community attributes (i.e., abundance, diversity and genus composition) were used as a proxy to evaluate the impact of the nodule collector, using a combination of morphological and metabarcoding methods. Besides the immediate-disturbance study, pre-impact samples obtained within the Trial site (i.e., Collector and Plume Impact sites) during two consecutive sampling campaigns (2019: SO268 and 2021: IP21) are compared to establish natural conditions of the abyssal nodule fields. Finally, recommendations for future DSM impact assessments on soft-sediment habitats are provided, based on our findings.

2 Material and methods

2.1 Study area

The Clarion-Clipperton Zone (CCZ) is an area of approximately 5.1 x 10^6 km^2 in the eastern equatorial Pacific Ocean, which has been designated by the ISA as a potential region for DSM due to its high abundance of high-grade (i.e., enriched in copper, nickel and cobalt) polymetallic nodules (Hein et al., 2013; Petersen et al., 2016). The exploration contract area of the Belgian company GSR is located in the north-eastern part of the CCZ, and the 72.728-km^2 large area is subdivided into three zones (Figure 1). The Trial site of the pre-prototype collector vehicle PATII was located in the central zone B4 (Figure 1), at the south-eastern flank of a 140-m high seamount in water depths of 4390-4530 m, exhibiting a nodule abundance of 20-24 kg/m^2 wet weight with a size of more than 4 cm, During the SO268 sampling campaign in 2019, baseline samples were also obtained within the Trial site (Haeckel and Linke, 2021).

2.2 Sediment plume monitoring

Prior to the PATII test (14-17 April 2021), an extensive sensor array for monitoring the sediment plume was installed on the seabed in the Trial area (Vink et al., 2022). It consisted of 20 sensor platforms with a total of 50 optical and acoustic sensors to monitor and quantify the spatiotemporal dynamics of the sediment plume created by PATII, together with two additional Sedimentation Level Indicator (SLIC) boxes to collect and measure the amount of resettled sediment. These devices were placed on the seabed by means of a Remotely Operated Vehicle (ROV) around the collector impact area (in a circle on a northwest-southeast axis) and at various distances (200 to 1000 m) along the south-southeast axis (Vink et al., 2022). This positioning corresponded with the expected sediment plume dispersal orientation, downslope of the dominant bathymetry gradient and downstream of the prevailing bottom currents, which was based on *a priori* predictive modelling as described by Purkiani et al. (2021).

2.3 Nodule mining trial

The nodule collection trial with PATII (dive number PAT009) in the GSR exploration contract area started on the 18th of April 2021. The vehicle was built at sub-industrial scale (1:4, 25 x 10^3 kg in

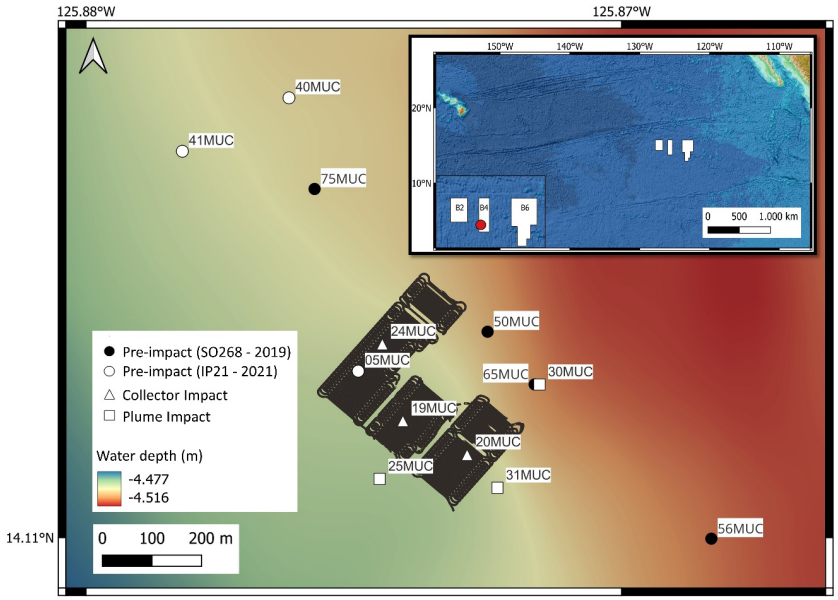

FIGURE 1
Map depicting the PATANIA II (PATII) tracks following a "fishtail" trajectory along three strips within the GSR exploration contract area, covering > 30.000 m^2. Symbols represent the location of the multicorer (MUC) sampling positions taken in the different categories: Pre-impact (SO268 and IP21), Collector Impact and Plume Impact cover. Upper right corner: location of the three zones (B2, B4 and B6) of the GSR exploration contract area in the northeastern part of the Clarion-Clipperton Zone. The red dot indicates the position of the PATII Trial site within B4.

water, L8 m x W4.8 m x H4.2 m) and is composed of a tracked propulsion (i.e., caterpillar tracks) and a hydraulic nodule collector system (https://deme-gsr.com/). The nodule collector vehicle was equipped with several sensors and cameras to monitor environmental conditions such as turbidity, current velocity and sedimentation. Nodules were collected in three strips along parallel 50-m long lanes following a continuous "fishtail" trajectory (Figure 1). Due to local seabed topography, the southernmost strip 1 and middle strip 2 could not be fully completed, resulting in a total of 55 and 31 lanes, respectively. The northernmost strip 3 had a more favorable topography and a total of 85 lanes were completed. Since no riser system was present to bring the nodules to the surface, collected nodules were stored in a container at the back of the PATII vehicle and deposited in the turns of the tracks. Discharge waste, composed of sediments and fragmented nodules, was returned to the seabed by a diffuser at the rear end of the vehicle. The mining trial ended on the 20th of April 2021 after a deployment on the seabed of approximately 40 hours in which approximately 6.6 x 10^5 kg of nodules were removed, from an area larger than 30.000 m^2 (Gazis et al., submitted)[1].

2.4 Soft sediment sample collection

A 20-core multicorer (MUC, Oktopus GmbH), equipped with 60 cm-long cores (inner diameter of 96 mm), was used to obtain soft sediment samples. Pre-impact or "no-impact" samples were obtained within the GSR Trial site throughout two consecutive sampling campaigns. During the SO268 campaign in 2019, four MUC deployments were performed along the northwest-southeast axis (Haeckel and Linke, 2021, Figure 1, Table 1). During the IP21 campaign (2021), one MUC deployment was performed prior to the trial (Figure 1; 05MUC). In addition, two deployments were taken after the trial, located at 500 m northwest of the impact site. This area was also considered as "undisturbed" due to the south-southeast dominated dispersal of the produced sediment plume, based on preliminary data from a turbidity sensor mounted on the AUV and a stationary sensor (NIOZ_PFM_05) placed at 200 m distance in between the MUC locations and the PATII trial site (Gazis et al., submitted)[1]. As such, both samples were categorized and further referred to as "Pre-impact" within this paper. This correct categorization could be confirmed after analyzing the AUV-based photo mosaics for plume deposition on the seafloor (Gazis et al., submitted)[1] and numerical modelling of the plume dispersion matching the sensor data (Purkiani and Haeckel, unpublished).

In addition, three MUC deployments were performed after the PATII trial during the IP21 campaign within the tracks of the PATII vehicle (Collector Impact, 1-3 days post-impact, Figure 1, Table 1). Samples were also obtained in the area adjacent to the collector test site (Plume Impact), subject to sedimentation (3-5 days post-impact, Figure 1, Table 1). The post-trial impact categorization (Collector Impact and Plume Impact) and positioning of the MUC deployments were chosen on board based on sensor readings (e.g., AUV and CTD-mounted sensors) and inspection of AUV/ROV derived imagery (Vink et al., 2022). From each deployment, 1-2 cores and 2-3 cores were allocated for meiofaunal morphological and metabarcoding analysis, respectively. Sediment was also collected from 2-3 cores during each deployment for environmental analyses. The exact amount of cores allocated for each type of analysis are provided in Appendix Table 1.

Processing of Pre-impact samples from the SO268 campaign are described in Lefaible et al. (2023) and are comparable to the methods used for the samples collected in IP21. The IP21 cores for meiofaunal analyses were photographed and stored on board at

TABLE 1 Multicorer (MUC) samples collected for environmental and meiofaunal analyses.

Sampling campaign	Sampling category	MUC deployment	Water depth (m)	Latitude (N)	Longitude (W)
SO268 (2019)	Pre-impact	50MUC	4507	14° 6.840′	125° 52.341′
SO268 (2019)	Pre-impact	56MUC	4501	14° 6.601′	125° 52.091′
SO268 (2019)	Pre-impact	65MUC	4495	14° 6.788′	125° 52.295′
SO268 (2019)	Pre-impact	75MUC	4495	14° 6.999′	125° 52.537′
IP21 (2021)	Pre-impact	05MUC	4495	14° 6.787′	125° 52.495′
IP21 (2021)	Pre-impact	40MUC	4496	14° 7.094′	125° 52.573′
IP21 (2021)	Pre-impact	41MUC	4493	14° 7.034′	125° 52.692′
IP21 (2021)	Collector Impact	19MUC	4493	14° 6.731′	125° 52.445′
IP21 (2021)	Collector Impact	20MUC	4498	14° 6.693′	125° 52.373′
IP21 (2021)	Collector Impact	24MUC	4491	14° 6.8173′	125° 52.468′
IP21 (2021)	Plume Impact	25MUC	4489	14° 6.666′	125° 52.471′
IP21 (2021)	Plume Impact	30MUC	4505	14° 6.772′	125° 52.292′
IP21 (2021)	Plume Impact	31MUC	4491	14° 6.656′	125° 52.339′

Samples are reported for each sampling campaign (2019: SO268 and 2021: IP21) per sampling category (Pre-impact, Collector Impact, Plume Impact), MUC deployment, water depth (m), and geographical location (coordinates in degrees, minutes).

4°C. The upper 0-5 cm layer were used for further morphological and metabarcoding analyses. Sediments were collected in plastic containers and fixed with 4% formaldehyde-seawater solution and 98% denatured ethanol for morphological and metabarcoding samples, respectively. Cores obtained for environmental analyses were sliced at different intervals depending on the type of variable under study. For the pigment measurements, cores were sliced at a 1 cm depth resolution (down to 20 cm depth), whereas cores were sliced at 0-1 cm, 1-5 cm and 5-10 cm sediment depth for the grain size, total organic carbon (TOC) and total nitrogen (TN) measurements. Sub-samples of 5 ml were taken for pigment analyses from each depth layer using a cut-off syringe, which was then sealed with a cap and wrapped in aluminum foil. Morphological samples were stored at room temperature, whilst metabarcoding and environmental samples were preserved at -20°C until transported to the Max Planck Institute for Marine Microbiology for pigment analysis (MPI-MM Bremen) and Ghent University for morphological, metabarcoding and environmental (grain size, TOC, TN) analyses.

2.4.1 Environmental samples

Granulometric data were obtained through laser diffraction using a Malvern Mastersizer HYDRO 2000. Sediment fraction classifications were done following Wenthworth (1992) and granulometric measurements included the median grain size (MGS, µm), together with the percentages of sand (> 63 µm), clay (< 4 µm) and silt (> 4 µm < 63 µm). Prior to nutrient analysis, sediments were homogenized and pre-treated with 1% HCl solution to remove inorganic carbon compounds. Percentages of total organic carbon (TOC, %) and total nitrogen (TN, %) were measured using an Element Analyzer Flash 2000 and were also used to calculate TOC : TN ratio's (C/N ratio) for each sample.

Pigment analysis for Chlorophyll-a (Chl-*a*) and phaeopigment concentrations was done using an acetone extraction method (Boetius and Damm, 1998). The sediment and 8 ml of cold acetone (90%) were transferred into Greiner tubes, containing six glass beads, and shaken in a cell mill for 3 min. The samples were then centrifuged at 1000 rpm for 10 min at 0°C, and the supernatants were transferred into new 15-ml tubes. Acetone was added two more times, and the supernatant was added to the 15-ml tube each time. After a last centrifugation step of the extract for 2 min at 1000 rpm and 0°C, 1 ml of the extract was transferred into a cuvette and measured at a Turner Trilogy fluorometer at an excitation wavelength of 428 nm and an emission wavelength of 671 nm. For the phaeopigment measurement, one drop of HCl (20%) was added to the extracts, which were then remeasured. The Chloroplast Pigment Equivalents (CPE, sum of Chl-*a* and phaeopigment concentration) was calculated for each sample, together with the percentage of Chl-*a* (Chl-*a* %, percentage of Chl-*a*:CPE ratio).

2.4.2 Meiofaunal morphological samples

The 0-5 cm sediment layer was rinsed with filtered tap water over a 32-µm sieve. Next, colloidal silica polymer Ludox HS-40 (density of 1.18 g/cm^3) was added to the remaining sediment and meiofaunal organisms were extracted through density-gradient centrifugation (3 x 12 min, at 1905 rcf) using a Hettich ROTANTA 460 R centrifuge. The resulting supernatant with meiofaunal organisms was then collected on a 32-µm sieve, fixed with 4% formaldehyde and stained with Rose Bengal. Further processing included the sorting, counting and higher-taxon identification of the meiofauna by means of a stereomicroscope. Meiofaunal counts were converted to abundance per surface area (ind./10 cm^2).

2.4.3 Meiofaunal metabarcoding samples

For a detailed description of the library preparation, we refer to the text box provided in the Supplementary Material.

2.4.3.1 Bioinformatic analyses

Gene-specific adapters were removed with Cutadapt v4.4 (Martin, 2011) as non-internal adapters with the following parameters: minimum length=1, maximum error rate=0.1, minimum overlap=5. Amplicon sequence variants (ASVs) were generated following the DADA2 tutorial (https://benjjneb.github.io/dada2/tutorial.html (Callahan et al., 2016)) with the exception that forward and reverse reads were truncated at 250 bp and 200 bp, respectively. Taxonomy was assigned to the ASVs with the ribosomal database project (RDP) classifier (Wang et al., 2007) in two steps: 1st a large reference sequence database was used containing 18991 sequences of eukaryotes and marine nematodes (from Silva release 123 99% Operational Taxonomic Units (OTUs) and UGent nematode Sanger sequences). In the second step, all ASVs receiving a "Nematoda" label where extracted, to these taxonomic assignment was completed using a smaller, marine-nematode-exclusive reference sequence database (971 sequences from Silva release 123 99% OTUs and UGent nematode Sanger sequences). The data were stored in a phyloseq object (McMurdie and Holmes, 2013) and rarefied to the lowest sequence count (n=9244) for further analyses. The R package Ampvis2 (Andersen et al., 2018) was used to visualize taxonomic composition. From the rarefied dataset, two alpha diversity indices were calculated, namely the number of ASVs corresponding to the ASV Richness and the ASV Shannon diversity.

2.5 Statistical analyses

Samples from one deployment (40MUC) were removed from the final biological IP21 dataset because sediment cores appeared highly disturbed after sampling. Final environmental datasets for the all the sampling categories were based on the mean of the pooled 0-5 cm sediment layers. Comparisons between the Pre-impact samples obtained during the two campaigns (SO268 vs. IP21) in terms of univariate environmental and meiofaunal properties were performed by means of independent t-tests. Since pigment measurements were done with different methods during each campaign, these variables were not included for the Pre-impact analysis.

For the immediate-disturbance study, univariate environmental and biological differences between the sampling categories from the IP21 campaign (i.e., Pre-impact, Collector Impact and Plume Impact) were assessed through a one-way analysis of variance

(ANOVA). Data normality and homoscedasticity were assessed by means of a Shapiro and Levene's test, respectively. If the ANOVA analysis was significant, Tukey post-hoc tests were performed to compare all possible pairs of groups/categories. In addition, power analyses were performed for the univariate community descriptors under study for the PATII impact assessment (IP21). Omega squared (ω^2) was chosen as a measure of effect size to quantify the magnitude of an effect, as it is considered to be a reliable estimate when sample sizes are small (Field, 2013). Firstly, ω^2 values were calculated based on the one-way ANOVA models of each variable, through the omega_squared() function and were classified as very small ($\omega^2 < 0.01$), small ($0.01 \leq \omega^2 < 0.06$), medium ($0.06 \leq \omega^2 < 0.14$) or large ($\omega^2 \geq 0.14$) according to Field (2013).

A one-way permutational analysis of variance (PERMANOVA, distance metric: unweighted UniFrac (Lozupone and Knight, 2005) was also applied to test for differences in terms of nematode ASV genus composition between Pre-impact sampling campaigns (SO268 vs. IP21) and impact categories during the IP21 campaign. Permdisp tests were performed to assess the homogeneity of multivariate dispersions. All statistical analyses and graphs were produced with R Statistical Software (v4.1.2; R Core Team 2021) using the following R packages: car (Fox and Weisberg, 2019), tidyverse (Wickham et al., 2019), vegan (Oksanen et al., 2019) and pwr (Champely, 2020).

3 Results

3.1 Trial site baseline conditions

3.1.1 Environmental variables

Average MGS was significantly higher (Figure 2, t-test, $p = 0.003$, Appendix Table 2) for the IP21 (2021) Pre-impact samples (20 ± 2 µm) compared to those from SO268 (2019) (17 ± 1 µm) and a similar pattern was found for the average sand fraction (IP21: 14 ± 3%, SO268: 12 ± 1%, Figure 2, t-test, $p = 0.03$). Clay fractions were also significantly lower for the IP21 Pre-impact samples (IP21: 13 ± 1%, SO268: 16 ± 1%, Figure 2, $p < 0.001$), while average silt fractions were comparable between both campaigns (Appendix Table 2, $p > 0.05$). Significant differences were also detected for the average TOC values and C/N ratio's, which were both higher in the IP21 Pre-impact samples (TOC: 0.55 ± 0.01%, C/N: 4.80 ± 0.23) relative to the Pre-impact samples from SO268 (TOC: 0.42 ± 0.01%, C/N: 2.73 ± 0.46) (Figure 2, TOC: $p = 0.002$ and C/N: $p < 0.001$). In contrast, average TN values were significantly higher (Figure 2, $p = 0.001$) for the SO268 sediments (0.16 ± 0.03%) compared to sediments obtained during IP21 (0.11 ± 0.02%) However, we would like to highlight that within-group variability was also observed, especially in terms of TOC values for the IP21 sediments and that granulometric differences between the campaigns were mainly

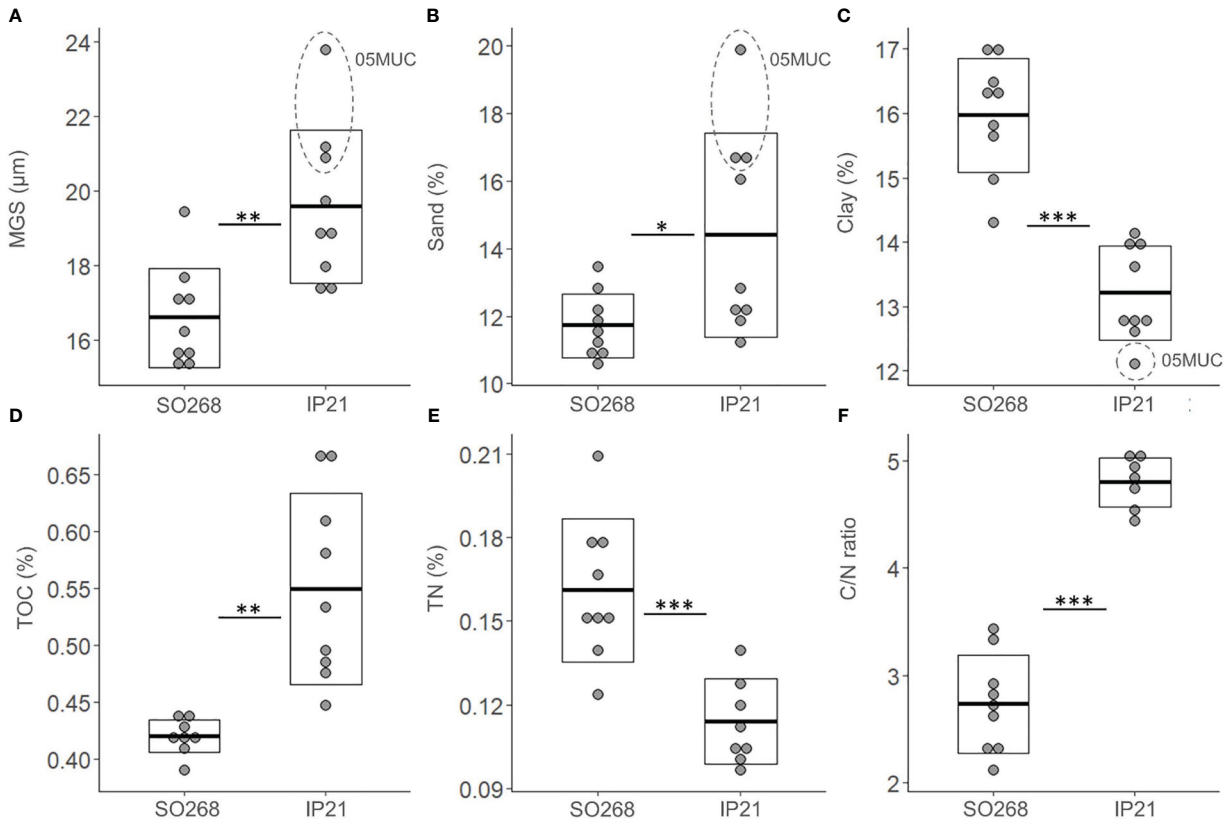

FIGURE 2
Environmental variables; **(A)** Median grain size (MGS, µm), **(B)** Sand fraction (Sand, %), **(C)** Clay fraction (Clay, %), **(D)** Total organic carbon (TOC, %), **(E)** Total nitrogen (TN, %) and **(F)** Total organic carbon to nitrogen ratio (C/N ratio) for the Pre-impact samples collected within the Trial site during the SO268 (2019) and IP21 (2021) campaigns. The crossbar and extent of the box represent the mean and standard deviation, respectively. Asterisks were added to visualize the p-values ($p < 0.05$ '*', $p < 0.01$ '**' and $p < 0.001$ '***') from the t-tests.

driven by measurements from one of the IP21 Pre-impact samples (05MUC, Figure 2).

3.1.2 Nematoda

Results from the t-tests showed that average total nematode abundance, ASV Richness and ASV Shannon diversity were comparable between samples from both campaigns (Appendix Table 2, $p > 0.05$, Appendix Figure 1). The genera *Acantholaimus* (> 20%), *Halalaimus* (≥ 16%), *Desmoscolex* (> 13%) and *Phanodermopsis* (> 10%) were the most abundant in the Pre-impact samples (Appendix Figure 2). However, nematode community composition differed significantly between the SO268 and IP21 campaign (one-way Permanova, $p = 0.002$ and Permdisp test, $p = 0.265$, Appendix Figure 3).

3.2 Impacts of the PATII trial

3.2.1 Environmental variables

All the granulometric variables showed comparable average values between categories (Table 2, one-way ANOVA's, $p > 0.05$). Sediments from the Collector Impact contained lower average TN relative to the Pre-impact and Plume Impact categories (Table 2), but these differences were not statistically significant ($p > 0.05$). In contrast, average TOC values showed statistically significant differences (Table 2, Figure 3, $p = 0.001$) and Tukey HSD post-hoc tests revealed that TOC was significantly lower in the Collector Impact (0.43 ± 0.04%) and Plume Impact (0.47 ± 0.03%) compared to the Pre-impact samples (0.55 ± 0.08%) (Figure 3, Pre-impact vs. Collector Impact, $p = 0.001$ and Pre-impact vs. Plume Impact, $p = 0.03$). The C/N ratios also differed between impact categories ($p = 0.021$) and were significantly lower for the Plume Impact samples (3.86 ± 0.28) compared to the Pre-impact samples (4.80 ± 0.23) (Figure 3, Tukey HSD test: pre-impact vs. Plume impact, $p = 0.016$).

Average Chl-*a* concentrations were similar for the Pre-impact and Plume Impact samples, while lower average values were found in the PATII tracks (Collector Impact) (Table 2), but no statistically significant difference was detected ($p > 0.05$). In terms of CPE, average values were significantly lower for the Collector Impact (0.030 ± 0.011 µg/ml) and Plume Impact (0.052 ± 0.022 µg/ml) samples compared to the Pre-impact samples (0.085 ± 0.029 µg/ml) (Figure 3) ($p = 0.001$ and Tukey HSD tests: Pre-impact vs. Collector Impact, $p = 0.001$ and Pre-impact vs. Plume Impact, $p = 0.01$). Average Chl-*a* % was highest within the Plume Impact (Table 2), but differences between categories were not statistically significant ($p > 0.05$).

3.2.2 Meiofauna

Considering all impact categories, Nematoda represented the dominant taxon in terms of relative abundance (94%), followed by Copepoda (4%). Polychaeta and nauplii (i.e., Crustacea larvae) both comprised about 1%, while other taxa such as Gastropoda, Isopoda, Tanaidacea, Halacarida and Kinorhyncha contributed to a lesser extent (< 0.1%). Differences between impact categories for

TABLE 2 Minimum (Min), maximum (Max), average and standard deviation (Av ± SD) of the abiotic and biotic variables in the 0-5cm sediment depth layer for each category (Pre-impact, Collector Impact and Plume Impact).

Environmental variables	Pre-impact			Collector Impact			Plume Impact		
	Min	Max	Av ± SD	Min	Max	Av ± SD	Min	Max	Av ± SD
MGS (µm)	17	24	20 ± 2	18	21	19 ± 1	17	23	19 ± 2
Sand (%)	11	20	14 ± 3	12	18	15 ± 2	13	24	17 ± 4
Silt (%)	68	75	72 ± 2	68	76	72 ± 3	63	72	69 ± 4
Clay (%)	12	14	13 ± 1	13	16	13 ± 1	12	15	14 ± 1
TN (%)	0.10	0.20	0.12 ± 0.03	0.07	0.13	0.10 ± 0.02	0.11	0.14	0.12 ± 0.01
TOC (%)	0.44	0.67	0.55 ± 0.08	0.38	0.47	0.43 ± 0.04	0.41	0.50	0.47 ± 0.03
C/N ratio	4.48	5.02	4.80 ± 0.23	3.48	5.84	4.37 ± 0.79	3.59	4.35	3.86 ± 0.28
Chl-a (µg/ml)	0.009	0.039	0.018 ± 0.010	0.002	0.035	0.011 ± 0.012	0.005	0.049	0.017 ± 0.012
CPE (µg/ml)	0.045	0.132	0.085 ± 0.029	0.012	0.045	0.030 ± 0.011	0.024	0.083	0.052 ± 0.022
Chl-a/CPE (%)	13	21	21 ± 7	4	98	39 ± 31	10	92	39 ± 29
Biological variables	**Pre-impact**			**Collector Impact**			**Plume Impact**		
	Min	Max	Av ± SD	Min	Max	Av ± SD	Min	Max	Av ± SD
TNAb (ind./10 cm^2)	7	145	71 ± 57	12	98	35 ± 34	9	168	90 ± 61
ASV Richness	35	297	145 ± 97	27	278	108 ± 73	50	256	143 ± 83
ASV Shannon diversity	3.18	4.05	3.55 ± 0.37	2.08	4.21	3.30 ± 0.69	3.29	4.43	3.85 ± 0.40

Granulometry: Median grain size (MGS, µm) and percent Silt/Clay (%). Nutrients: Total nitrogen (TN, %), Total organic carbon (TOC, %) and Total organic carbon to Nitrogen ration (C/N ratio). Pigments: Chlorophyll-a (Chl-a, µg/ml), Chloroplastic Pigment Equivalents (CPE, µg/ml) and percent of Chl-a/CPE ratio (Chl-a %, %). Biotic indices: Total Nematoda Abundance (TNAb, ind./10 cm^2), Number of Nematoda Amplicon Sequence Variants (ASVs) corresponding to the ASV Richness and ASV Shannon diversity.

10.3389/fmars.2024.1380530

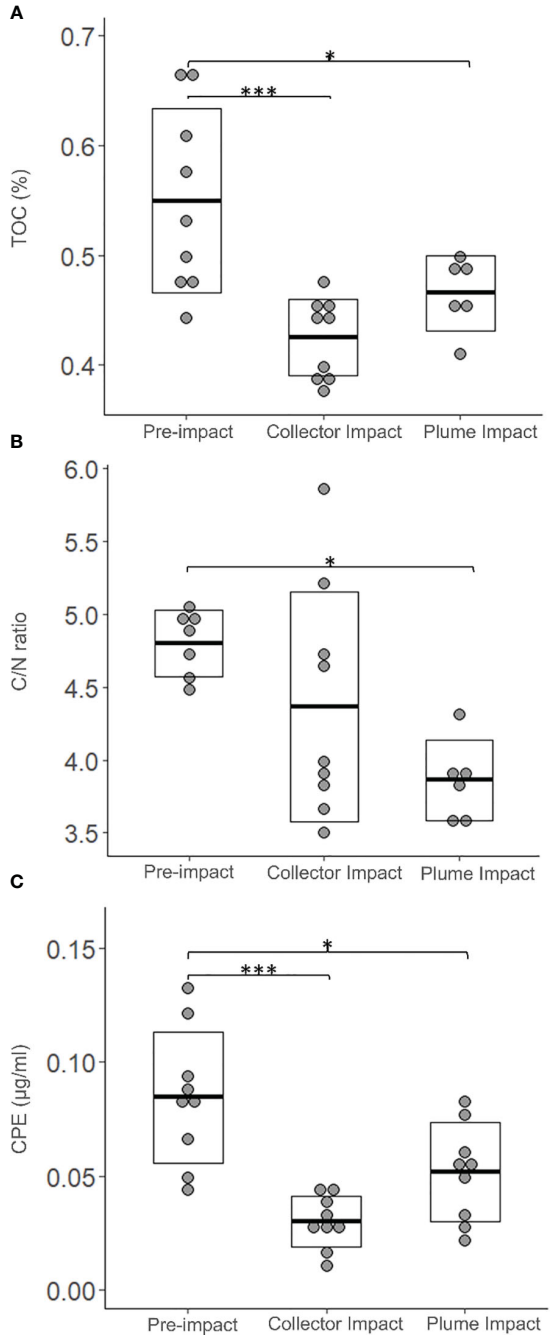

FIGURE 3
Environmental variables; **(A)** Total organic carbon (TOC, %), **(B)** Total organic carbon to Nitrogen ration (C/N ratio) and **(C)** Chloroplast Pigment Equivalent (CPE, µg/ml) for each category sampled during the IP21 campaign (Pre-impact, Collector Impact, Plume Impact) along the 0-5 cm sediment depth layer. The crossbar and extent of the box represent the mean and standard deviation, respectively. Asterisks were added if Tukey HSD post-hoc tests were significant ($p < 0.05$ '*' and $p < 0.001$ '***').

Nematoda abundance, diversity and genus composition are described in detail within the following section. For the remaining more important taxa, Copepoda and Polychaeta were found to be more abundant in the post-impact categories compared to the Pre-impact samples, while an opposite patterns was seen for nauplii (Appendix Figure 4). However, no statistically significant differences were detected for these three taxa in terms of average abundances between impact categories ($p > 0.05$).

3.2.2.1 Nematode abundance and ASV diversity

Average total Nematoda abundance was highest for the Plume Impact samples and a comparable result was found for the ASV Shannon diversity (Table 2, Figure 4). In terms of ASV Richness, averages values were quite similar for the Pre-impact and Plume Impact samples, while lowest average ASV Richness was observed within the Collector impact samples. However, all biological indices showed considerable variability within each category (Table 2, Figure 4) and differences between the three categories were not statistically significant ($p > 0.05$). Post-hoc power analyses for the statistical test for the difference in total Nematoda abundance between impact categories (one-way ANOVA with factor "category") revealed that the test had a medium to large effect size and that a total of 33 samples would be required within each category to achieve a desired statistical power of 0.80 (alpha = 0.05, $\omega^2 = 0.09$, groups = 3). For the Nematoda ASV Shannon diversity, comparable results were found with a medium to large effect size and a required sample size of n = 30 for each category to obtain a statistical power of 0.80 ($\alpha = 0.05$, $\omega^2 = 0.10$, groups = 3). In contrast, power analysis was not possible for the Nematoda ASV species richness, as the calculated effect size was equal to zero.

3.2.2.2 Nematoda community composition

The most abundant nematode genus across all three impact categories was *Acantholaimus*, representing ≥ 15% of the assemblage by relative read abundance (Figure 5). *Halalaimus*, *Desmoscolex* and *Chromadorita* also represented abundant genera in all categories, albeit with varying relative read abundance (4-15%). Other important genera included *Phanodermopsis* (4-11%) and *Theristus* (3-4%) in the Pre-impact and Plume Impact samples, while they showed much lower read numbers in the Collector Impact samples (< 0.5%) (Figure 5). It has to be mentioned that both genera were not shared among all the category samples, with higher relative abundance restricted to one or two MUC deployments. The genera *Syringolaimus* and *Tripyloides* also showed considerable relative read abundances (5-6%) within the Collector Impact samples. *Tripyloides* was exclusively found in this impact category, but was only present in 20MUC. Within the Plume Impact samples, the genus *Anticoma*, represented 5% of the assemblage, while much lower read numbers (< 0.5%) of *Anticoma* were found for the other categories (Figure 5). This genus occurred in the majority of the Plume Impact samples, except for 25MUC. Many other genera contributed to a lesser extent (< 5%) to the overall nematode assemblage (Figure 5). However, no statistically significant differences were found in terms of Nematode ASV genus composition between impact categories (one-way Permanova, $p > 0.05$ and Permdisp test: $p = 0.03$).

4 Discussion

4.1 Abyssal nodule-rich sediments

Abyssal sediments in the CCZ area are characterized as fine-grained, mainly consisting of clay and silt, rich in manganese-oxide (MnO_2) (Pape et al., 2017; Hauquier et al., 2019; Volz et al., 2020). Primary productivity in the surface waters of the CCZ is oligotrophic, resulting in low particulate organic carbon (POC) fluxes to the seafloor (< 2 mg $C_{org}m^{-2}d^{-1}$) (Lutz et al., 2007; Volz et al., 2018a). Pre-impact upper sediments (0-5 cm) within our study site exhibited environmental properties (e.g., silt > 70%, clay < 20%, TN < 0.2% and TOC < 0.6%), comparable with previously described baseline conditions in the GSR exploration contract area (De Smet et al., 2017; Pape et al., 2017; Volz et al., 2018; Hauquier et al., 2019). Deep-sea nematode assemblages tend to be characterized by a few prevailing and many rare taxa (Lambshead and Boucher, 2003; Pape et al., 2017; Hauquier et al., 2019; Lefaible et al., 2023). This pattern was also observed in our study, with highest relative read abundance for the genera *Acantholaimus* and *Halalaimus*, which are commonly reported as dominant in nodule-bearing abyssal sediments (Pape et al., 2017; Hauquier et al., 2019; Macheriotou et al., 2020; Lefaible et al., 2023). Previous metabarcoding studies further corroborated that *Desmoscolex*, *Chromadorita* and *Phanodermopsis* are also important genera in terms of relative read abundance (> 5%) in the CCZ (Macheriotou et al., 2020; Lefaible et al., 2023).

Nevertheless, significant geochemical and biological differences were found between baseline sediments taken at the Trial site during two consecutive campaigns (i.e., SO268 and IP21). Stations sampled immediately prior to the PATII trial (Pre-impact IP21) were characterized by significantly higher TOC contents and labile organic matter fractions (C/N ratios) then those sampled during SO268. Differences in food availability may be a consequence of temporal variation in seafloor POC flux but lateral heterogeneity in TOC has also been attributed to interactions between bottom-water currents, topographic relief (e.g., basins, ridges) and the degree of organic matter degradation (Lutz et al., 2007; Volz et al., 2018a; Vonnahme et al., 2020). Since benthic fauna in abyssal sediments is driven by sediment composition and food availability, it can be expected that spatial differences in these variables will also result in spatially patchy meiofaunal communities (Lambshead and Boucher, 2003; Pape et al., 2017; Hauquier et al., 2019; Kuhn et al., 2020; Washburn et al., 2019). Next to this natural heterogeneity on a larger spatial scale (i.e., between sampling stations), abyssal sediments and especially meiofaunal communities are known to exhibit small-scale heterogeneity even between cores of the same deployment (Rosli et al., 2018; Uhlenkott et al., 2021; Lefaible et al., 2023), which was also observed within this study.

For example, average nematode abundances of the Pre-impact IP21 samples varied considerably, ranging from 7 up to 145ind./10 cm^2. This high degree of variability regarding nematode abundance is probably also linked to the presence of polymetallic nodules, as they represent the only natural hard substrate in these areas and will therefore influence local habitat complexity, which is considered to be an additional driver of benthic faunal distribution (Vanreusel et al., 2010; Zeppilli et al., 2016; Uhlenkott et al., 2021). A very low number of nematodes (7 ind./10 cm^2) occurred in one core sample that contained a large, superficial nodule, whereas higher (≥ 140 ind./10 cm^2) to moderate (60-70 ind./10 cm^2) abundances were observed in cores containing smaller nodules, located in deeper sediment layers (Appendix Figure 5). Reduced nematode abundance has consistently been found in nodule-rich areas compared to nodule-free areas (e.g. Miljutina et al., 2010; Singh and Ingole, 2016; Pape et al., 2017; Hauquier et al., 2019; Pape et al., 2021; Uhlenkott et al., 2021) and it has been proposed that a negative relationship between nodule presence and faunal abundance exists due to reduced sediment volume for nematodes (Pape et al., 2017; Hauquier et al., 2019). While the current increase in deep-sea research will provide better understanding of baseline conditions in proposed mining areas, we would like to emphasize that the high level of natural heterogeneity observed in our study has strong implications for effective impact assessments and distinguishing anthropogenic disturbances from natural variability (see section 4.3).

4.2 DSM-induced pressures

Studies such as ours, in which a sub-industrial scale vehicle was used, will be crucial to perform detailed DSM impact assessments and quantify the spatio-temporal extent of the effects that are induced during nodule collection. Therefore, the most pronounced DSM effects in the form of sediment removal, seabed alterations and enhanced sediment deposition are discussed separately throughout the following sections (4.2.1, 4.2.2) in an attempt to identify the mechanisms behind the different stressors and the associated meiofaunal responses. Based on our findings, we also provide methodological recommendations for future DSM research on benthic habitats (4.3).

4.2.1 Sediment removal and seabed alterations

The productive surface sediments in abyssal areas contain the bulk of food-associated compounds such as the labile organic matter pool and biota including meiofaunal organisms (Boetius and Haeckel, 2018; Volz et al., 2020; Vonnahme et al., 2020). Consequently, removal of this ecologically important bioactive layer during nodule mining is considered as one of the most severe DSM pressures, expected to alter meiofaunal distribution, biogeochemical processes and overall ecosystem functioning (Thiel, 2001; Boetius and Haeckel, 2018). Comparable to previous small-scale benthic impact experiments (Volz et al., 2020; Vonnahme et al., 2020; Lefaible et al., 2023), TOC and CPE concentrations in our study were significantly lower in the Collector Impact tracks relative to undisturbed Pre-impact samples, which suggests that sediment removal resulted in the reduction of food sources for benthic organisms in the form of fresh and more refractory organic matter (Volz et al., 2020). Although not significant, average nematode abundance and ASV diversity was also observed to decrease in parallel with the environmental changes in the directly impacted

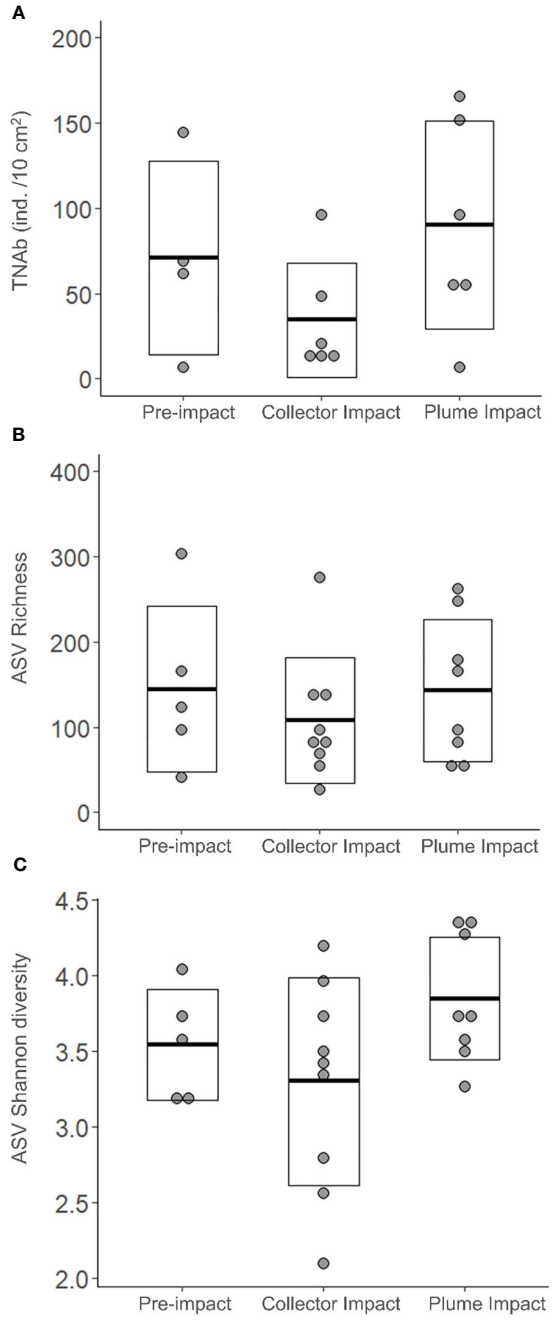

FIGURE 4
Biological univariate variables: **(A)** Total Nematoda Abundance (TNAb, ind. /10 cm2), **(B)** Number of Nematoda Amplicon Sequence Variants (ASVs) corresponding to the ASV Richness and **(C)** ASV Shannon diversity for each category sampled during the IP21 campaign (Pre-impact, Collector Impact, Plume Impact). The crossbar and extent of the box represent the mean and standard deviation, respectively.

sediments, which is accordance with previously reported meiofaunal responses in most of the available benthic impact studies (Jones et al., 2018).

Despite the fact that there were no significant differences between categories in terms of nematode ASV genus composition, our results suggest that sediments within the PATII tracks contained less *Halalaimus* while *Syringolaimus* was more abundant. Both genera are commonly found in the deep-sea, but *Syringolaimus* has been observed more frequently in environmentally extreme environments (e.g., sediments close to hydrothermal vents) and is believed to be more resistant to stress compared to *Halalaimus* (Zeppilli et al., 2015). *Syringolaimus* has also been described as nodule-associated with higher relative abundances inside nodule crevices compared to surrounding soft-sediment (Pape et al., 2021). Consequently, individuals of this genus might also be released into the exposed sediments due to nodule breakdown during the collection process. Moreover, *Triplyloides* was exclusively found in the Collector Impact samples. This observation is difficult to explain as this group is less common within deep-sea abyssal sediments and occurrences were restricted to one sampling station. Shallow-water studies state that this genus is an epistrate feeder, predating on ciliates (Bongers et al., 1991; Moens and Vincx, 1997; Moens et al., 2013) and has also been shown to show a negative correlation with Chlorophyll *a* concentrations (Moens et al., 1999). This finding, in combination with the fact that this genus is virtually absent in Pre-impact sediments, may indicate that it represents a colonizing taxon in the freshly disturbed sediments. However, whether this represents an active response must be confirmed by results of the follow-up study (SO295 campaign, 2022).

Our findings confirm the hypothesis that the hydraulic system used during nodule collection resulted in the removal of considerable fractions of the upper sediments (a minimum of 5 cm, Gazis et al., submitted)[1]. However, our study also shows that in addition to sediment removal, complex and variable seabed alterations were created by the propulsion system of the collector vehicle. Seabed imagery obtained after the PATII trial revealed that the sediment patches in the wake of the collector vehicle are characterized by two main topographic features (Figure 6). First, there is a centrally located sediment strip, defined by relatively homogeneous sediment removal and upper layer topography. Secondly, the edges of tracks are manifested as parallel sediment strips with caterpillar imprints composed by alternating bands of depressions and ripples with the presence of unstable sediment clumps on top of the ripples and at the interface between the depressions and ripples (Figure 6). Vonnahme et al. (2020) already differentiated several microhabitats such as outside the track, subsurface/exposed patches, ridges and furrows based on visual observations in a 26-year old plough and a fresh (2.5 weeks) epibenthic sledge (EBS) track in the DISCOL Experimental Area in the Peru Basin. Several classes of disturbances were described, representing a gradient of environmental impact ranging from low (outside the tracks) to severe (removal of active surface layer) with variable microbial responses in each microhabitat (Vonnahme et al., 2020).

This variability in environmental disturbance implies that the degree of impact and associated meiofaunal responses will depend on the exact sampling position within the Collector Impact tracks, which was confirmed by a visual inspection of the high-resolution images of the sediment cores taken for morphological analysis (Appendix Figure 6). Sample 24MUC was TV-guided and one of the cores contained the lowest nematode abundance (12 ind./10 cm^2), corresponding to a highly impacted area in the caterpillar depressions, where the dark, MnO_2-rich layer was almost

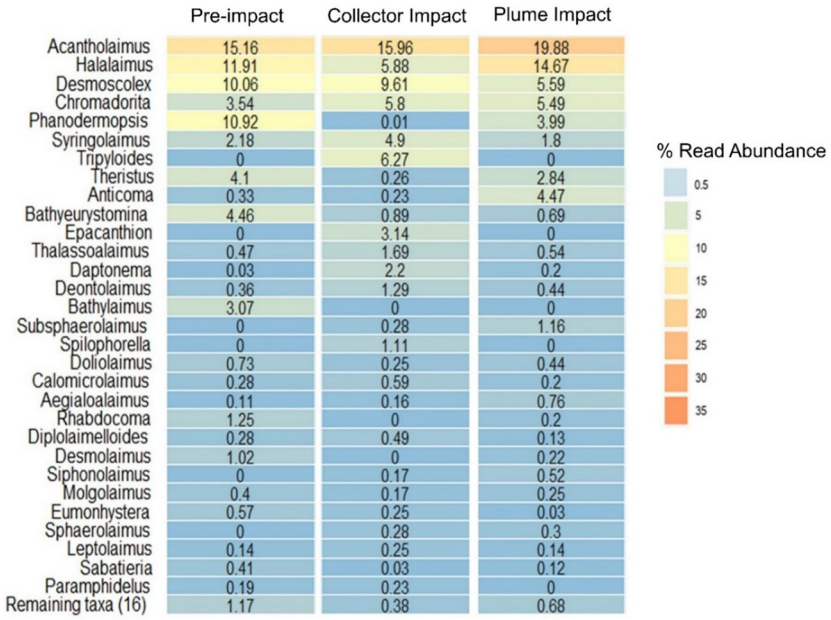

FIGURE 5
Heat map with the relative read abundance (%) of genus-assigned Nematoda Amplicon Sequence Variants (ASVs) for each category sampled during the IP21 campaign (Pre-impact, Collector Impact, Plume Impact).

completely removed (Appendix Figure 6 and Table 3). In contrast, another core from the same MUC deployment had relatively high nematode abundance (98 ind./10 cm^2) and showed an irregular surface relief with sediment clumps, indicating that this sample may have been taken within a ripple of the caterpillar profile (Appendix Figure 6 and Table 3). For the remaining deployments, exact sampling positions remain uncertain, but the qualitative description of the high-resolution images and AUV-derived photomosaics suggest that samples from 20MUC might have been taken at an interface patch at the edge between a depression/ripple with low nematode abundances (≤ 20 ind./10 cm^2). Moreover, varying nematode abundances (15-50 ind./10 cm^2) were observed in samples with relatively homogenous sediment removal corresponding with the sediment strips between caterpillar imprints. These findings demonstrate that nodule collection will induce different sediment modification types on relatively small spatial scales (~meter), with biological responses dependent on the type and intensity of disturbance.

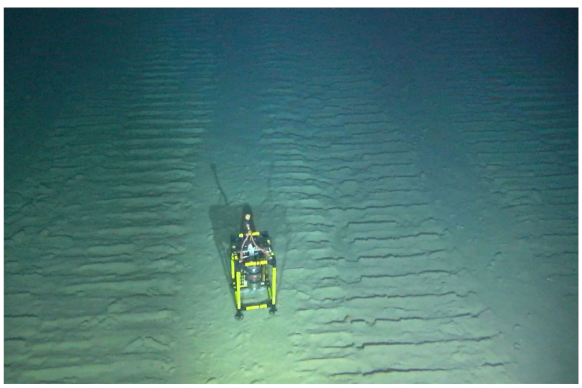

FIGURE 6
High-resolution image taken with the Remotely Operated Vehicle (ROV, IP21_044ROV1, photo credit: BGR) during the IP21 campaign within the Collector Impact site.

4.2.2 Collector-induced sediment plumes

Investigating the impacts of enhanced sedimentation on benthic habitats represents one of the biggest challenges within DSM research. This is mainly due to the dynamic character of the collector-induced sediment plumes, as they are influenced by many factors such as the nodule collection and separation methods, local seabed topography, sediment properties and hydrodynamic conditions (e.g., background turbidity, currents and near-bottom mixing) (Purkiani et al., 2021; Haalboom et al., 2022; Helmons et al., 2022; Muñoz-Royo et al., 2022; Gazis et al., submitted)[1]. Nevertheless, enormous progress has been made in recent years in the techniques needed to characterize plume dispersal patterns (Purkiani et al., 2021; Haalboom et al., 2022; Helmons et al., 2022; Muñoz-Royo et al., 2022; Gazis et al., submitted)[1]. Preliminary results from the plume monitoring and geochemistry analyses during the PATII trial showed that sediment dispersal occurred in a relatively narrow band along the predominant current direction. Sediment blanketing (2-3 cm) was observed up to ~100 m from the Collector Impact site, becoming thinner with distance and was not visible on AUV photos anymore beyond 2 km (Vink et al., 2022; Gazis et al., submitted)[1].

4.2.2.1 Blanketing outside collector tracks

Compared to Pre-impact conditions, samples collected within the Plume Impact site showed significantly higher CPE values and

enhanced nematode abundance and ASV diversity, although these increases in community metrics were not significant different. These patterns are consistent with a small-scale disturbance (i.e., modelled sedimentation < 1 cm) experiment in the CCZ, where most pronounced meiofaunal enrichment was reported for limited modelled blanketing (< 3 mm) (Lefaible et al., 2023). Moreover, visual inspection of the high-resolution images of the sediment cores obtained for morphological analysis allowed us to approximate the level of sediment deposition in the form of changes in grain/flocculation size, or presence of black grained nodule material, and link this with the observed nematode abundances. This further confirmed that thickness of the deposited sediment was around 2-3 cm for the majority of the samples, with nematode abundance ranging from relatively high (≥ 150 ind./10 cm^2) to moderate (60-100 ind./10 cm^2). While our results verify that surrounding areas were subject to considerable blanketing, we want to emphasize that there are still many uncertainties regarding the geochemical and biological changes associated with anthropogenically-induced sedimentation.

For example, it was expected that the redeposition of the reactive sediment surface layers from the Collector Impact sites in the Plume Impact sites would result in higher or comparable food availability. In contrast, average CPE, TOC values and C/N ratios were significantly lower within the Plume Impact areas compared to Pre-impact sediments. It is known that sediment blanketing occurs in a gradual manner, with fractionation of the resettling particles with rapid deposition of heavier particles (Gillard et al., 2019; Purkiani et al., 2021; Muñoz-Royo et al., 2022). However, it remains unclear for now what influence the aggregate type or flocculation material of the plume (e.g., grain size and organic particle composition) will have on vertical element fluxes such as organic carbon absorption with the surface matrix and concomitant animal-sediment interactions (e.g., microbial-mediated degradation, benthic bioturbation and burrowing) (Haeckel et al., 2001; Arndt et al., 2013; Bianchi et al., 2021).

Mechanisms driving the observed nematode enrichment in the Plume Impact area are also currently unresolved but probable scenarios include either active upward migration of organisms from the original surface sediment now covered by the sediment from the plume, or deposition of suspended surface sediments present in the plume, or a combination of both (Mevenkamp et al., 2017, 2019; Lefaible et al., 2023). In the latter case, it is, however, unknown whether upward migration or deposition is the main contributor to the overall faunal fraction in adjacent sediments and to what extent the resettled fauna within the so-called "blanket" represent damaged/dead or alive organisms (Lefaible et al., 2023). Answering these important questions is further complicated by the sampling interval of 0-5 cm used in our study. Since the collector-induced sediment deposition thickness was approximately 2-3 cm, environmental and biological patterns in this study represent an integrated result from the blanketing layer and exposed, natural sediments.

4.2.2.2 Blanketing inside collector tracks

Rapid redeposition of the suspended particle plume was detected after the PATII trial (Gazis et al., submitted)[1] within the tracks, which corroborates findings from a numerical modelling analysis after a small-scale disturbance experiment (Gillard et al., 2019; Purkiani et al., 2021). Layers of discharged sediment and ground nodule material were also observed for the majority of our high-resolution images of the Collector Impact samples (Appendix Figure 6). However, the level of blanketing thickness appears to vary depending on the exact position in the collector lanes with stronger sediment accumulation in the caterpillar depressions compared to the ripples (Gazis et al., submitted)[1]. Depressions generated during a plough disturbance experiment, showed a low-density layer of deposited sediment and it was suggested that these furrows might act as an accumulation spot for particle resettlement (Vonnahme et al., 2020). The fact that these sediments within the Collector Impact site are subject to a sequence of multiple pressures (sediment removal, intricate seabed modification by collector vehicle and heavy blanketing) enhances the complexity with which mined areas will be affected. However, examining cumulative stressors is very difficult and it remains unclear whether the combination of collector-induced physical seabed disturbances and sediment deposition will result in additive, antagonistic or synergistic impacts on meiofaunal communities (Carrier-Belleau et al., 2021).

4.3 Future challenges: quantifying multiple sources of variability

The comparison of environmental conditions within the Pre-impact and post-impact categories of our study confirm the hypothesis that a considerable fraction of the upper sediment layer within the collector impact site was removed (a minimum of 5 cm, Gazis et al., submitted)[1] during nodule collection and that surrounding areas were subject to sediment blanketing (± 2-3 cm). Although average values (i.e., reduced levels in Collector Impact sites, enhanced in Plume Impact sites) for the Nematoda community indices support that environmental changes will also have impacts on the associated biota, differences between categories were not statistically significant. Post-hoc power analyses did, however, reveal that nematode abundance and ASV Shannon diversity tests were characterized by moderate to strong effect sizes, indicating the biological relevance of changes in these variables (Field, 2013). Moreover, univariate biological tests had low statistical power and a substantial increase in samples size (n = 30 per category) would be required to achieve appropriate statistical sensitivity (power level 80%). As such we propose that the lack of significant biological results might be attributed to the insufficient replication combined with noticeable within-category variability. This conclusion further illustrates what can be considered as the main challenge of DSM research, namely: quantifying multiple sources of variability associated with i) the intricate collector-induced seabed disturbances and ii) the natural heterogeneity of abyssal sediments (Clark et al., 2020).

Nodule collection by the PATII vehicle induced a sequence of pressures (i.e., sediment removal, intricate seabed modification by collector vehicle and sediment blanketing), resulting in complex seabed modifications with different disturbance types such as i) central lanes of sediment removal, ii) alternating bands of

depressions/ripples in caterpillar tracks, ii) microscale variations in topography due to unstable sediment "clumps" and varying levels of sediment deposition in the Collector Impact site. It will therefore be necessary to distinguish and integrate these disturbances into the data collection of future benthic DSM studies. A proposed solution would be to apply a nested sampling design within the "Collector Impact" category, where sufficient replication is performed for the major subgroups (e.g., central lanes, depressions and ripples of caterpillar profile). It could also be opted to combine MUC samples with ROV push cores, which are taken in a more targeted manner owing to the live camera feed. As shown in this study, *a priori* methods like the visual inspection of high-resolution images from the collected samples can help to determine specific seabed alterations (e.g., estimation of position in PATII tracks, exact sedimentation level). Whereas our results indicate that both post-impact categories were affected by enhanced sedimentation, many uncertainties remain regarding the effects of sediment blanketing on overall seabed integrity. Regarding meiofaunal responses, one very important aspect will be to find methods (e.g., staining, DNA/RNA techniques) to determine whether the assemblages were alive or not at time of sampling. Moreover, continued monitoring will be crucial to identify the long term viability of the present populations.

Environmental and biological properties of the Pre-impact samples in our study fell within the range of previously described baseline conditions in the same area. Nevertheless, heterogeneity across small and large spatial scales has been a consistent pattern in the CCZ. As such, an important implication is that environmental variables should preferably be obtained from the same samples used for biological analyses. Furthermore, the sediment depth resolution (i.e., entire 0-5 cm layer) used in this study was not appropriate to distinguish redeposited from natural sediments in adjacent areas (i.e., Plume Impact category) where sediment blanketing was up to 3 cm. Therefore, it should be explored if it is feasible to adjust the slicing depth resolution of the core samples, depending on the expected sediment deposition thickness. Furthermore, we want to emphasize that findings in our study reflect immediate (i.e., one week after trial) benthic responses, and results from the follow-up SO295 campaign will provide additional insights on how the benthic environment has evolved over a period of 1.5 year (MI2, 2018). Lastly, given the observed inter-annual variability in terms of environmental and faunal baseline conditions in our study. Understanding natural temporal variability based on adequate time series and a sufficiently high number of replicates of abyssal benthic communities is therefore crucial for establishing and predicting the impacts of mining activities in deep-sea ecosystems.

5 Conclusions

Significantly lower total organic carbon, CPE (i.e., sum of Chlorophyll *a* and phaeopigments), and patterns of impoverished nematode assemblages within the Collector Impact area were observed in our study, which supports the hypothesis that nodule collection by PATII removed the ecologically important bioactive surface layer. Besides this seabed alteration, impacted areas also experienced sediment blanketing (2-3 cm), with higher accumulation in caterpillar depressions, indicating different spatial intensities of disturbance. Collector-induced sediment blanketing occurred in adjacent areas outside the Collector Impact area, with sediment deposition up to 3 cm. These Plume Impact sediments exhibited lower food availability, and further research on the plume composition's role in biogeochemical processes is needed. Mechanisms driving observed meiofaunal enrichment at Plume Impact sites (albeit not statistically significant), and the extent to which deposited fauna represent living individuals remain unclear. We conclude that DSM activities will affect benthic communities in a complex manner and with varying biological responses. These conclusions, together with the spatial and temporal variability in terms of Pre-impact conditions, highlight that future impact studies should incorporate increased replication, larger spatial coverage and long-term monitoring to address uncertainties and distinguish anthropogenic disturbances from natural variability in abyssal polymetallic nodule fields.

Data availability statement

The datasets presented in this study can be found in online repositories. The names of the repository/repositories and accession number(s) can be found below: https://doi.org/10.1594/PANGAEA.941222, https://doi.org/10.1594/PANGAEA.941216, https://doi.pangaea.de/10.1594/PANGAEA.942156, https://doi.org/10.1594/PANGAEA.942177, https://doi.org/10.1594/PANGAEA.952416, https://doi.org/10.1594/PANGAEA.952333.

Ethics statement

The manuscript presents research on animals that do not require ethical approval for their study.

Author contributions

NL: Methodology, Formal analysis, Writing – original draft. LM: Methodology, Formal analysis, Writing – review & editing. EP: Writing – review & editing. MM: Methodology, Writing – review & editing. MH: Project administration, Funding acquisition, Writing – review & editing. DZ: Writing – review & editing. AV: Project administration, Funding acquisition, Writing – review & editing.

Funding

The author(s) declare financial support was received for the research, authorship, and/or publication of this article. This

research has been supported by the Department of Economy, Science and Innovation of Flanders (grant no. 0248.015.142), the German Federal Ministry of Education and Research BMBF (grant no. 03F0812A-G) in the framework of JPI Oceans project MiningImpact 2 and the DEEP REST project that was funded through the 2020-2021 Biodiversa and Water JPI joint call for research projects, under the BiodivRestore ERA-NET Cofund (grant no. 101003777). DZ was supported by the by the Ifremer Marine Mineral Resources project (REMIMA project) and by the French National Research Agency under France 2030 (reference ANR-22-MAFM-0001).

Acknowledgments

We would like to express our gratitude to the captain and crew of the SO268 and IP21 sampling campaigns. A special thanks to Freija Hauquier and Jolien Goossens for their participation during the sample collection. We would also like to thank Bart Beuselinck and Bruno Vlaeminck for processing the environmental variables and Annick Van Kenhove for her assistance with the meiofaunal morphological samples. All sample processing at Ghent University within this study was possible due to the facilities and material provided by EMBRC (GOH3817N).

Conflict of interest

The authors declare that the research was conducted in the absence of any commercial or financial relationships that could be construed as a potential conflict of interest.

The author(s) declared that they were an editorial board member of Frontiers, at the time of submission. This had no impact on the peer review process and the final decision.

Publisher's note

Supplementary material

The Supplementary Material for this article can be found online at: https://www.frontiersin.org/articles/10.3389/fmars.2024.1380530/full#supplementary-material

References

Amon, D. J., Gollner, S., Morato, T., Smith, C. R., Chen, C., Christiansen, S., et al. (2022). Assessment of scientific gaps related to the effective environmental management of deep-seabed mining. *Mar. Policy* 138, 105006. doi: 10.1016/j.marpol.2022.105006

Andersen, K. S., Kirkegaard, R. H., Karst, S. M., and Albertsen, M. (2018). ampvis2: an R package to analyse and visualise 16S rRNA amplicon data. doi: 10.1101/299537

Arndt, S., Jørgensen, B. B., LaRowe, D. E., Middelburg, J. J., Pancost, R. D., and Regnier, P. (2013). Quantifying the degradation of organic matter in marine sediments: A review and synthesis. *Earth-Science Rev.* 123, 53–86. doi: 10.1016/j.earscirev.2013.02.008

Bianchi, T. S., Aller, R. C., Atwood, T. B., Brown, C. J., Buatois, L. A., Levin, L. A., et al. (2021). What global biogeochemical consequences will marine animal-sediment interactions have during climate change? *Elementa* 9, 1–25. doi: 10.1525/elementa.2020.00180

Boetius, A., and Damm, E. (1998). Benthic oxygen uptake, hydrolytic potentials and microbial biomass at the Arctic continental slope. *Deep. Res. Part I Oceanogr. Res. Pap.* 45, 239–275. doi: 10.1016/S0967-0637(97)00052-6

Boetius, A., and Haeckel, M. (2018). Mind the seafloor. *Science* 359, 34–36. doi: 10.1126/science.aap7301

Bongers, T., Alkemade, R., and Yeates, G. W. (1991). Interpretation of disturbance-induced maturity decrease in marine nematode assemblages by means of the Maturity Index. *Mar. Ecol. Prog. Ser.* 76, 135–142. doi: 10.3354/meps076135

Broadus, J. M. (1987). Seabed materials. *Science* 235, 853–860. doi: 10.1126/science.235.4791.853

Callahan, B. J., McMurdie, P. J., Rosen, M. J., Han, A. W., Johnson, A. J. A., and Holmes, S. P. (2016). DADA2: high-resolution sample inference from Illumina amplicon data. *Nat. Methods* 13, 581583. doi: 10.1038/nmeth.3869

Carrier-Belleau, C., Drolet, D., McKindsey, C. W., and Archambault, P. (2021). Environmental stressors, complex interactions and marine benthic communities' responses. *Sci. Rep.* 11, 1–14. doi: 10.1038/s41598-021-83533-1

Champely, S. (2020) *Pwr: Basic Functions for Power Analysis*. Available at: https://CRAN.R-project.org/package=pwr.

Clark, M. R., Durden, J. M., and Christiansen, S. (2020). Environmental Impact Assessments for deep-sea mining: Can we improve their future effectiveness? *Mar. Policy* 114, 103363. doi: 10.1016/j.marpol.2018.11.026

Danovaro, R., and Gambi, C. (2022). Cosmopolitism, rareness and endemism in deep-sea marine nematodes. *Eur. Zool. J.* 89, 653–665. doi: 10.1080/24750263.2022.2040621

De Smet, B., Pape, E., Riehl, T., Bonifácio, P., Colson, L., and Vanreusel, A. (2017). The community structure of deep-sea macrofauna associated with polymetallic nodules in the eastern part of the Clarion-Clipperton Fracture Zone. *Front. Mar. Sci.* 4. doi: 10.3389/fmars.2017.00103

Field, A. (2013). *Discovering statistics using IBM SPSS Statistics. 4th ed.* (London: Sage).

Fox, J., and Weisberg, S. (2019) *An R Companion to Applied Regression*. Available at: https://socialsciences.mcmaster.ca/jfox/Books/Companion/index.html.

Gillard, B., Purkiani, K., Chatzievangelou, D., Vink, A., Iversen, M. H., and Thomsen, L. (2019). Physical and hydrodynamic properties of deep sea mining-generated, abyssal sediment plumes in the Clarion Clipperton Fracture Zone (eastern-central Pacific). *Elementa* 7, 5. doi: 10.1525/elementa.343

Haalboom, S., Schoening, T., Urban, P., Gazis, I. Z., de Stigter, H., Gillard, B., et al. (2022). Monitoring of anthropogenic sediment plumes in the clarion-clipperton zone, NE equatorial pacific ocean. *Front. Mar. Sci.* 9. doi: 10.3389/fmars.2022.882155

Haeckel, M., König, I., Riech, V., Weber, M. E., and Suess, E. (2001). Pore water profiles and numerical modelling of biogeochemical processes in Peru Basin deep-sea sediments. *Deep. Res. Part II Top. Stud. Oceanogr.* 48, 3713–3736. doi: 10.1016/S0967-0645(01)00064-9

Haeckel, M., and Linke, P. (2021). RV SONNE cruise report SO268 - assessing the impacts of nodule mining on the deep-sea environment: noduleMonitoring. *GEOMAR Rep.* 59, 802. doi: 10.3289/GEOMAR_REP_NS_59_20

Haffert, L., Haeckel, M., De Stigter, H., and Janssen, F. (2020). Assessing the temporal scale of deep-sea mining impacts on sediment biogeochemistry. *Biogeosciences* 17, 2767–2789. doi: 10.5194/bg-17-2767-2020

Hallgren, A., and Hansson, A. (2021). Conflicting narratives of deep sea mining. *Sustain.* 13, 1–20. doi: 10.3390/su13095261

Hasemann, C., Mokievsky, V., Sablotny, B., Tekman, M. B., and Soltwedel, T. (2020). Effects of sediment disturbance on deep-sea nematode communities: Results from an in-situ experiment at the arctic LTER observatory HAUSGARTEN. *J. Exp. Mar. Bio. Ecol.* 533, 151471. doi: 10.1016/j.jembe.2020.151471

Hauquier, F., Macheriotou, L., Bezerra, T., Egho, G., Martínez Arbizu, P., and Vanreusel, A. (2019). Distribution of free-living marine nematodes in the clarion-clipperton zone: Implications for future deep-sea mining scenarios. *Biogeosciences* 16, 3475–3489. doi: 10.5194/bg-16-3475-2019

Hein, J. R., Mizell, K., Koschinsky, A., and Conrad, T. A. (2013). Deep-ocean mineral deposits as a source of critical metals for high- and green-technology applications: Comparison with land-based resources. *Ore Geol. Rev.* 51, 1–14. doi: 10.1016/j.oregeorev.2012.12.001

Helmons, R., de Wit, L., de Stigter, H., and Spearman, J. (2022). Dispersion of benthic plumes in deep-sea mining: what lessons can be learned from dredging? *Front. Earth Sci.* 10. doi: 10.3389/feart.2022.868701

Jones, D. O. B., Amon, D. J., and Chapman, A. S. A. (2018). Mining deep-ocean mineral deposits: What are the ecological risks? *Elements* 14, 325–330. doi: 10.2138/gselements.14.5.325

Jones, D. O. B., Kaiser, S., Sweetman, A. K., Smith, C. R., Menot, L., Vink, A., et al. (2017). Biological responses to disturbance from simulated deep-sea polymetallic nodule mining. *PloS One* 12 (2), e0171750. doi: 10.1371/journal.pone.0171750

König, I., Haeckel, M., Lougear, A., Suess, E., and Trautwein, A. X. (2001). A geochemical model of the Peru Basin deep-sea floor - And the response of the system to technical impacts. *Deep. Res. Part II Top. Stud. Oceanogr.* 48, 3737–3756. doi: 10.1016/S0967-0645(01)00065-0

Kuhn, T., Uhlenkott, K., Vink, A., Rühlemann, C., and Martinez Arbizu, P. (2020). Manganese nodule fields from the Northeast Pacific as benthic habitats. *Seafloor Geomorphol. as Benthic Habitat* 58, 933–947. doi: 10.1016/B978-0-12-814960-7.00058-0

Lambshead, P. J. D., and Boucher, G. (2003). Marine nematode deep-sea biodiversity - Hyperdiverse or hype? *J. Biogeogr.* 30, 475–485. doi: 10.1046/j.1365-2699.2003.00843.x

Lefaible, N., Macheriotou, L., Purkiani, K., Haeckel, M., Zeppilli, D., Pape, E., et al. (2023). Digging deep: lessons learned from meiofaunal responses to a disturbance experiment in the Clarion-Clipperton Zone. *Mar. Biodivers.* 53, 48. doi: 10.1007/s12526-023-01353-0

Lozupone, C., and Knight, R. (2005). UniFrac: a new phylogenetic method for comparing microbial communities. *Appl. Environ. Microbiol.* 71, 82288235.

Lutz, M. J., Caldeira, K., Dunbar, R. B., and Behrenfeld, M. J. (2007). Seasonal rhythms of net primary production and particulate organic carbon flux to depth describe the efficiency of biological pump in the global ocean. *J. Geophys. Res. Ocean.* 112, C10011. doi: 10.1029/2006JC003706

Macheriotou, L., Rigaux, A., Derycke, S., and Vanreusel, A. (2020). Phylogenetic clustering and rarity imply risk of local species extinction in prospective deep-sea mining areas of the Clarion–Clipperton Fracture Zone. *Proc. R. Soc B Biol. Sci.* 287 (1924), 20192666. doi: 10.1098/rspb.2019.2666

Martin, M. (2011). Cutadapt removes adapter sequences from high-throughput sequencing reads. *EMBnet. J.* 17, 10–12. doi: 10.14806/ej.17.1.200

McMurdie, P. J., and Holmes, S. (2013). Phyloseq: An R Package for Reproducible Interactive Analysis and Graphics of Microbiome Census Data. *PloS One* 8 (4), e61217. doi: 10.1371/journal.pone.0061217

Mevenkamp, L., Guilini, K., Boetius, A., De Grave, J., Laforce, B., Vandenberghe, D., et al. (2019). Responses of an abyssal meiobenthic community to short-term burial with crushed nodule particles in the south-east Pacific. *Biogeosciences* 16, 2329–2341. doi: 10.5194/bg-16-2329-2019

Mevenkamp, L., Stratmann, T., Guilini, K., Moodley, L., van Oevelen, D., Vanreusel, A., et al. (2017). Impaired short-term functioning of a benthic community from a deep Norwegian fjord following deposition of mine tailings and sediments. *Front. Mar. Sci.* 4. doi: 10.3389/fmars.2017.00169

Miljutin, D. M., Miljutina, M. A., Arbizu, P. M., and Galéron, J. (2011). Deep-sea nematode assemblage has not recovered 26 years after experimental mining of polymetallic nodules (Clarion-Clipperton Fracture Zone, Tropical Eastern Pacific). *Deep. Res. Part I Oceanogr. Res. Pap.* 58, 885–897. doi: 10.1016/j.dsr.2011.06.003

Miljutina, M. A., Miljutin, D. M., Mahatma, R., and Galéron, J. (2010). Deep-sea nematode assemblages of the Clarion-Clipperton Nodule Province (Tropical North-Eastern Pacific). *Mar. Biodivers.* 40, 1–15. doi: 10.1007/s12526-009-0029-0

Miller, K. A., Brigden, K., Santillo, D., Currie, D., Johnston, P., and Thompson, K. F. (2021). Challenging the need for deep seabed mining from the perspective of metal demand, biodiversity, ecosystems services, and benefit sharing. *Front. Mar. Sci.* 8. doi: 10.3389/fmars.2021.706161

MiningImpact2 (MI2) (2018). *Environmental impacts and risks of deep-sea mining: proposal.* 64.

Moens, T., Braeckman, U., Derycke, S., Fonseca, G., Gallucci, F., Gingold, R., et al. (2013). Ecology of free-living marine nematodes. *Handbook of zoology : Gastrotricha, Cycloneuralia and Gnathifera* 2, 109-152. doi: 10.1515/9783110274257.109

Moens, T., Van Gansbeke, D., and Vincx, M. (1999). Linking estuarine nematodes to their suspected food. A case study from the Westerschelde Estuary (south-west Netherlands). *J. Mar. Biol. Assoc. United Kingdom* 79, 1017–1027. doi: 10.1017/S0025315499001253

Moens, T., and Vincx, M. (1997). Observations on the feeding ecology of estuarine nematodes. *J. Mar. Biol. Assoc. United Kingdom* 77, 211–227. doi: 10.1017/S0025315400033889

Muñoz-Royo, C., Ouillon, R., El Mousadik, S., Alford, M. H., and Peacock, T. (2022). An in *situ* study of abyssal turbidity-current sediment plumes generated by a deep seabed polymetallic nodule mining preprototype collector vehicle. *Sci. Adv.* 8 (38), eabn1219. doi: 10.1126/sciadv.abn1219

Oebius, H. U., Becker, H. J., Rolinski, S., and Jankowski, J. A. (2001). Parametrization and evaluation of marine environmental impacts produced by deep-sea manganese nodule mining. *Deep. Res. Part II Top. Stud. Oceanogr.* 48, 3453–3467. doi: 10.1016/S0967-0645(01)00052-2

Oksanen, J., Simpson, G. L., Blanchet, F. G., Kindt, R., Legendre, P., Minchin, P. R., et al. (2019) *vegan: Community Ecology Package. R package version 2.5–6.* Available at: https://CRAN.R-project.org/package=vegan.

Pape, E., Bezerra, T. N., Gheerardyn, H., Buydens, M., Kieswetter, A., and Vanreusel, A. (2021). Potential impacts of polymetallic nodule removal on deep-sea meiofauna. *Sci. Rep.* 11, 1–15. doi: 10.1038/s41598-021-99441-3

Pape, E., Bezerra, T. N., Hauquier, F., and Vanreusel, A. (2017). Limited spatial and temporal variability in meiofauna and nematode communities at distant but environmentally similar sites in an area of interest for deep-sea mining. *Front. Mar. Sci.* 4. doi: 10.3389/fmars.2017.00205

Petersen, S., Krätschell, A., Augustin, N., Jamieson, J., Hein, J. R., and Hannington, M. D. (2016). News from the seabed – Geological characteristics and resource potential of deep-sea mineral resources. *Mar. Policy* 70, 175–187. doi: 10.1016/j.marpol.2016.03.012

Purkiani, K., Gillard, B., Paul, A., Haeckel, M., Haalboom, S., Greinert, J., et al. (2021). Numerical simulation of deep-sea sediment transport induced by a dredge experiment in the northeastern Pacific Ocean. *Front. Mar. Sci.* 8. doi: 10.3389/fmars.2021.719463

R Core Team (2021). *R: A Language and Environment for Statistical Computing.* Vienna: R Foundation for Statistical Computing. Available at: https://www.R-project.org.

Rex, M. A., Etter, R. J., Morris, J. S., Crouse, J., McClain, C. R., Johnson, N. A., et al. (2006). Global bathymetric patterns of standing stock and body size in the deep-sea benthos. *Mar. Ecol. Prog. Ser.* 317, 1–8. doi: 10.3354/meps317001

Rosli, N., Leduc, D., Rowden, A. A., and Probert, P. K. (2018). Review of recent trends in ecological studies of deep-sea meiofauna, with focus on patterns and processes at small to regional spatial scales. *Mar. Biodivers.* 48, 13–34. doi: 10.1007/s12526-017-0801-5

Singh, R., and Ingole, B. S. (2016). Structure and function of nematode communities across the Indian western continental margin and its oxygen minimum zone. *Biogeosciences* 13, 191–209. doi: 10.5194/bg-13-191-2016

Sparenberg, O. (2019). A historical perspective on deep-sea mining for manganese nodules 1965–2019. *Extr. Ind. Soc* 6, 842–854. doi: 10.1016/j.exis.2019.04.001

Stratmann, T., Lins, L., Purser, A., Marcon, Y., Rodrigues, C. F., Ravara, A., et al. (2018). Abyssal plain faunal carbon flows remain depressed 26 years after a simulated deep-sea mining disturbance. *Biogeosciences* 15, 4131–4145. doi: 10.5194/bg-15-4131-2018

Thiel, H. (2001). Evaluation of the environmental consequences of polymetallic nodule mining based on the results of the TUSCH Research Association. *Deep. Res. Part II Top. Stud. Oceanogr.* 48, 3433–3452. doi: 10.1016/S0967-0645(01)00051-0

Uhlenkott, K., Vink, A., Kuhn, T., Gillard, B., and Arbizu, P. M. (2021). Meiofauna in a potential deep-sea mining area—influence of temporal and spatial variability on small-scale abundance models. *Diversity* 13, 1–16. doi: 10.3390/d13010003

Vanreusel, A., Fonseca, G., Danovaro, R., Da Silva, M. C., Esteves, A. M., Ferrero, T., et al. (2010). The contribution of deep-sea macrohabitat heterogeneity to global nematode diversity. *Mar. Ecol.* 31, 6–20. doi: 10.1111/j.1439-0485.2009.00352.x

Vanreusel, A., Hilario, A., Ribeiro, P. A., Menot, L., and Arbizu, P. M. (2016). Threatened by mining, polymetallic nodules are required to preserve abyssal epifauna. *Sci. Rep.* 6, 1–6. doi: 10.1038/srep26808

Vink, A., Aigner, T., Bardenhagen, M., Barz, J., Bouriat, A., Charlet, F., et al. (2022). *MANGAN 2021 Cruise Report. Federal Institute for Geosciences and Resources* (Hannover, Germany), 370. p. doi: 10.25928/hw7d-fs42

Volz, J. B., Haffert, L., Haeckel, M., Koschinsky, A., and Kasten, S. (2020). Impact of small-scale disturbances on geochemical conditions, biogeochemical processes and element fluxes in surface sediments of the eastern Clarion-Clipperton Zone, Pacific Ocean. *Biogeosciences* 17, 1113–1131. doi: 10.5194/bg-17-1113-2020

Volz, J. B., Mogollón, J. M., Geibert, W., Arbizu, P. M., Koschinsky, A., and Kasten, S. (2018). Natural spatial variability of depositional conditions, biogeochemical processes and element fluxes in sediments of the eastern Clarion-Clipperton Zone, Pacific Ocean. *Deep. Res. Part I Oceanogr. Res. Pap.* 140, 159–172. doi: 10.1016/j.dsr.2018.08.006

Vonnahme, T. R., Molari, M., Janssen, F., Wenzhöfer, F., Haeckel, M., Titschack, J., et al. (2020). Effects of a deep-sea mining experiment on seafloor microbial communities and functions after 26 years. *Sci. Adv.* 6 (18), eaaz5922. doi: 10.1126/sciadv.aaz5922

Wang, Q., Garrity, G. M., Tiedje, J. M., and Cole, J. R. (2007). Naıve Bayesian classifier for rapid assignment of rRNA sequences into the new bacterial taxonomy. *Appl. Environ. Microbiol.* 73, 52615267. doi: 10.1128/AEM.00062-07

Washburn, T. W., Turner, P. J., Durden, J. M., Jones, D. O. B., Weaver, P., and Van Dover, C. L. (2019). Ecological risk assessment for deep-sea mining. *Ocean Coast. Manage.* 176, 24–39. doi: 10.1016/j.ocecoaman.2019.04.014

Wickham, H., Averick, M., Bryan, J., Chang, W., McGowan, L., François, R., et al. (2019). Welcome to the tidyverse. *J. Open Source Software* 4, 1686. doi: 10.21105/joss.01686

Wilber, D. H., and Clarke, D. G. (2001). Biological effects of suspended sediments: A review of suspended sediment impacts on fish and shellfish with relation to dredging activities in estuaries. *North Am. J. Fish. Manage.* 21, 855–875. doi: 10.1577/1548-8675(2001)021<0855:beossa>2.0.co;2

Zeppilli, D., Pusceddu, A., Trincardi, F., and Danovaro, R. (2016). Seafloor heterogeneity influences the biodiversity-ecosystem functioning relationships in the deep sea. *Sci. Rep.* 6 (1), 26352. doi: 10.1038/srep26352

Zeppilli, D., Vanreusel, A., Pradillon, F., Fuchs, S., Mandon, P., James, T., et al. (2015). Rapid colonisation by nematodes on organic and inorganic substrata deployed at the deep-sea Lucky Strike hydrothermal vent field (Mid-Atlantic Ridge). *Mar. Biodivers.* 45, 489–504. doi: 10.1007/s12526-015-0348-2